

Precipitate pattern formation in fluctuating media

Ferenc Izsák^{a)}

Department of Applied Analysis, Eötvös University, P.O. Box 120, Budapest H-1518, Hungary

István Lagzi^{b)}

Department of Physical Chemistry, Eötvös University, P.O. Box 32, Budapest H-1518, Hungary

(Received 8 October 2003; accepted 28 October 2003)

Simulation of the Liesegang pattern formation in low concentration gradient is presented using concentration perturbation in a deterministic model. The precipitation process is based on ion-product supersaturation theory (Ostwald's model). In the classical experiments with high initial concentration gradients, appearance time and locations of the band formation are well reproducible. Decreasing initial concentration gradients results in a more stochastic pattern structure; this means that the reproducibility of the experiments becomes worse. The presented model and the results of the simulations exhibit the same trend, which were demonstrated and investigated experimentally by Kai *et al.* [S. Kai, S. C. Müller, and J. Ross, *J. Phys. Chem.* **87**, 806 (1983)] and Kai and Müller [S. Kai and S. C. Müller, *Sci. Form* **1**, 9 (1985)]. © 2004 American Institute of Physics.
[DOI: 10.1063/1.1635354]

I. INTRODUCTION

In some reaction-diffusion systems the precipitate forms patterns; this fact has been observed and published for the first time by Liesegang.¹ The quasiperiodic precipitation patterns appear due to interdiffusion of the two, initially separated electrolytes. One of them is in gel (inner electrolyte), the other one (outer electrolyte) diffuses from outside. The evolution of the bands is highly influenced by the initial concentration gradient: the concentration of the outer electrolyte determines the distance of the bands (measured from the junction point of the two electrolytes). This regularity is described by the Matalon–Packter law,^{2,3}

$$p \sim \frac{1}{a_0},$$

at fixed initial concentration b_0 of the inner electrolyte, where a_0 denotes that of the outer electrolyte. $1+p$ is the spacing coefficient: the ratio of the distances of the consecutive bands.⁴

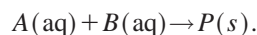
On the other hand, low initial concentration difference ($\Delta = a_0 - b_0$) leads to considerable uncertainty, in terms of the location of bands and of the appearance time. In real experiments^{5–7} the authors pointed out that pattern formation exhibits increasingly stochastic behavior as Δ approaches to zero. To interpret their results, they applied statistical analysis by fitting Gaussian functions to the detected bands. In many cases, the position of the bands far from the gel surface fluctuated such that the fitting procedure could not be performed. All of these provoked us to choose a stochastic approach in order to describe the phenomenon. The models, proposed in the literature, were either microscopic or macroscopic. For a general approach of modeling chemical pro-

cesses we refer to Ref. 8. Microscopic (or discrete) models treat the reacting particles individually both in the diffusion process and in the reactions. These sophisticated models contain the inherent fluctuation of the system and provide a detailed description of the precipitation process. Therefore, they give us a true description of the stochastic behavior of pattern formation.^{9–12} On the other hand, these models are realistic only, if a great number of particles are taken and this requirement leads to high computational cost. Macroscopic (mean field) models of Liesegang pattern formation focus on the concentrations $a(t,x)$, $b(t,x)$ of the outer and the inner electrolytes, respectively.^{13–22} Although these models are deterministic, we can modify them in order to take into consideration some stochastic effects, like fluctuation of concentrations—usually caused by heat anomalies, inhomogeneities of the gel structure or contaminations in the gel. Accordingly, Antal *et al.* developed a model based on a Cahn–Hilliard-type phase separation. They used a kinetic Ising model, which incorporated microscopic fluctuations.²³

The objective of the present study is to perturb the concentrations in a certain deterministic model in such a way that it reflects the increasingly stochastic behavior at low values of Δ . We will explain in the frame of our model the experimental results of Kai *et al.*,⁵ Kai and Müller,⁶ and Müller and Ross,⁷ and reproduce them numerically.

II. MODEL

The basic processes in systems that show regular Liesegang pattern formation are simple. The diffusive reagents (outer and inner electrolytes) A and B turn into an immobile precipitate P as



To describe the precipitate formation we have chosen the deterministic model proposed by Büki *et al.*^{18,19} based on the Ostwald's supersaturation theory²⁴ (ion-product supersatura-

^{a)}Also at Department of Applied Mathematics, University of Twente. Electronic mail: bizsu@cs.elte.hu

^{b)}Electronic mail: lagzi@vuk.chem.elte.hu

tion theory). Experiments are usually carried out in a gel matrix: the role of the gel is to prevent sedimentation of the precipitate and convection. Therefore, evolution of such systems in 1D can be described by the following reaction-diffusion equations—all quantities are dimensionless,

$$\frac{\partial a}{\partial \tau} = D_a \frac{\partial^2 a}{\partial x^2} - \delta(ab, K, L), \quad (1a)$$

$$\frac{\partial b}{\partial \tau} = D_b \frac{\partial^2 b}{\partial x^2} - \delta(ab, K, L), \quad (1b)$$

$$\frac{\partial p}{\partial \tau} = \delta(ab, K, L), \quad (1c)$$

where a , b , and p are the concentrations of the outer and the inner electrolyte and the amount of the precipitate depending on time (τ) and space variable (x). D_a and D_b denote the diffusion coefficients of the electrolytes. $\delta(ab, K, L)$ is the precipitation reaction term defined as follows:

If $p=0$ (there is no precipitate)

$$\delta(ab, K, L) = \kappa S_p \Theta(ab - K),$$

if $p>0$ (there is some precipitate)

$$\delta(ab, K, L) = \kappa S_p \Theta(ab - L),$$

where κ is the rate constant of the precipitation reaction, L is the solubility product, K is the nucleation product and Θ is the Heaviside step function. S_p is the amount of the precipitate which can form, defined as follows (proposed by Büki *et al.*^{18,19}):

$$S_p = \frac{1}{2} [(a+b) - \sqrt{(a+b)^2 - 4(ab-L)}].$$

The basis of the model is that precipitation occurs only if the product of the concentrations reaches K . However, if previously formed precipitate is present, it promotes the precipitation process and product of the concentrations has to reach only a lower threshold L . In our calculations we did not limit the amount of the precipitate at any space position. The above equations (1a)–(1c) are deterministic, but we suppose that the concentration of both electrolytes consists of two parts:

$$a = \bar{a} + a' \quad \text{and} \quad b = \bar{b} + b', \quad (2)$$

where \bar{a} , \bar{b} are the average concentrations, while a' , b' yield the concentration fluctuations. Variations of fluctuations $\partial a'/\partial \tau$ and $\partial b'/\partial \tau$ are usually considered to be zero since the average effect of these terms for any time interval is zero. Inserting Eq. (2) into Eqs. (1a)–(1c) gives

$$\frac{\partial \bar{a}}{\partial \tau} = D_a \frac{\partial^2 (\bar{a} + a')}{\partial x^2} - \delta((\bar{a} + a')(\bar{b} + b'), K, L), \quad (3a)$$

$$\frac{\partial \bar{b}}{\partial \tau} = D_b \frac{\partial^2 (\bar{b} + b')}{\partial x^2} - \delta((\bar{a} + a')(\bar{b} + b'), K, L), \quad (3b)$$

$$\frac{\partial p}{\partial \tau} = \delta((\bar{a} + a')(\bar{b} + b'), K, L). \quad (3c)$$

During the computation process, first the concentration of the two electrolytes were perturbed, then the diffusion and the

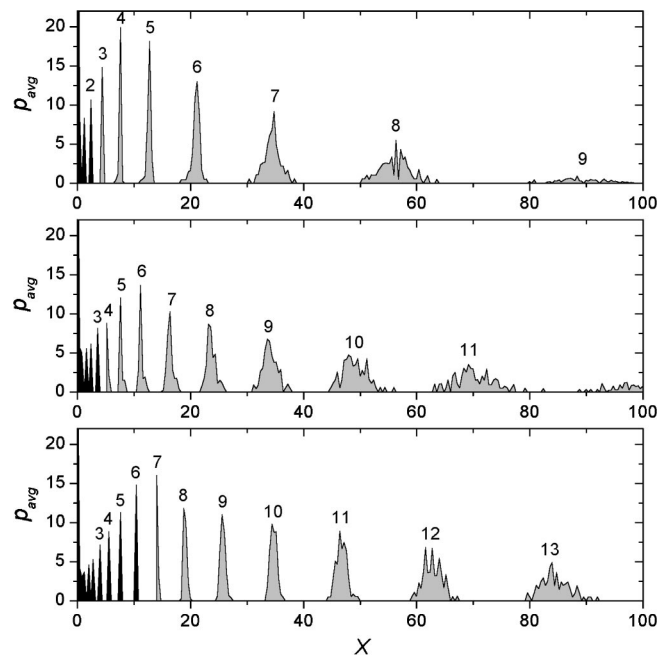


FIG. 1. Variation of the average amount of the precipitate in the diffusion column for $\Delta=0.0$ (top), $\Delta=0.4$ (middle), and $\Delta=0.8$ (bottom). The distribution of the precipitate corresponds to the average from 100 independent simulations. The black and gray color correspond to the deterministic and the stochastic band positions, respectively.

reaction terms were consecutively calculated with the perturbed concentrations. This process has been repeated in every time step. Perturbation a' of \bar{a} (perturbation b' of \bar{b}) can be described as the summed up random effects acting on each particles (of type A and B). We suppose that all of them have 0 mean and the same variance. The central limit theorem implies, that the sum of the effects has 0 mean, and its variance is proportional to the square root of the number of particles, i.e., that of the concentration. Therefore, we calculated the perturbation of concentrations as follows:

$$a' = (0.5 - \text{rand}(x, \tau)) d \sqrt{\bar{a}}, \quad (4a)$$

$$b' = (0.5 - \text{rand}(x, \tau)) d \sqrt{\bar{b}}, \quad (4b)$$

where d is related to the magnitude of the fluctuations and $\text{rand}(x, \tau)$ is a normally distributed random number between 0 and 1. It has been generated for the different electrolytes in every position in each time step.

Equations (3a)–(3c) have been solved numerically using a second order Runge–Kutta method with the following boundary conditions:

$$\left. \frac{\partial a}{\partial x} \right|_{x=0} = a_0 \quad \text{and} \quad \left. \frac{\partial b}{\partial x} \right|_{x=0} = \left. \frac{\partial a}{\partial x} \right|_{x=l} = \left. \frac{\partial b}{\partial x} \right|_{x=l} = 0,$$

where l is the length of the diffusion column. In all simulations we used the parameter set $D_a = D_b = 0.4$, $K = 0.13$, $L = 0.1$, $\kappa = 250.0$, $l = 480$, and $d = 0.0003$. The initial conditions were

$$a(0, x) = a_0 \Theta(-x), b(0, x) = b_0 \Theta(x) \quad \text{and} \quad p(0, x) = 0.$$

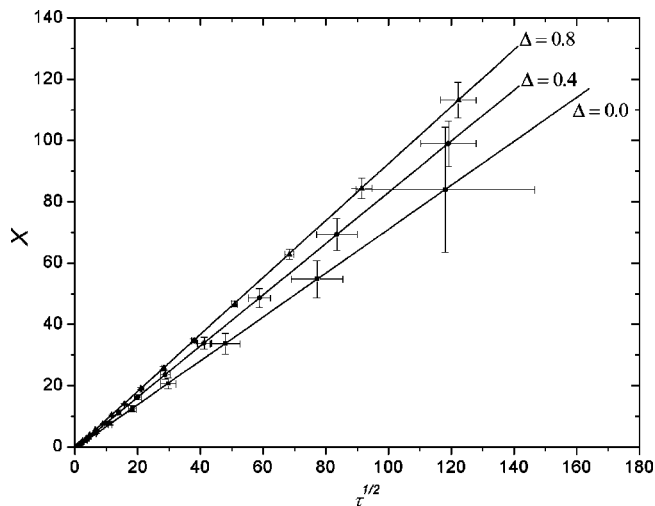


FIG. 2. Dependence of the average distance of bands (measured from the junction point of the two electrolytes) on the average square root of appearance time with the spatial and square root time standard deviations of 100 simulations. The solid lines are the fitted linear curves for the different values of Δ .

Here we chose $b_0=1.0$, while a_0 was varied between 1.0 and 1.8. The grid spacing was $\Delta x=0.4$ and we performed numerical simulations with the time step $\Delta \tau=0.004$.

III. RESULTS AND DISCUSSIONS

Figure 1 shows the empirical density function of band locations along the diffusion column at various initial concentration differences of the two electrolytes (Δ). We presented the average of 100 calculations. One can see clearly that decreasing Δ , the spatial distribution of band system becomes more stochastic. Note that although decreasing Δ leads to smaller perturbations (4a)–(4b), at the same time the pattern exhibits more stochastic behavior. We called a precipitate band position stochastic, if after the averaging process this band occupies more than one spatial grid cell, which arises from the spatial discretization of the partial differential equations (3a)–(3b). Bands occupying one spatial grid cell after the averaging process were considered to be deterministic. Figure 2 reflects this trend more evidently. This figure displays the verification of the time law,²⁵ which states the linear dependence of distance of the bands on the square root of it's formation time. Standard deviation of the band positions and square root of formation times increase during the development of patterns. Both standard deviations decrease with increasing Δ . These two main observations

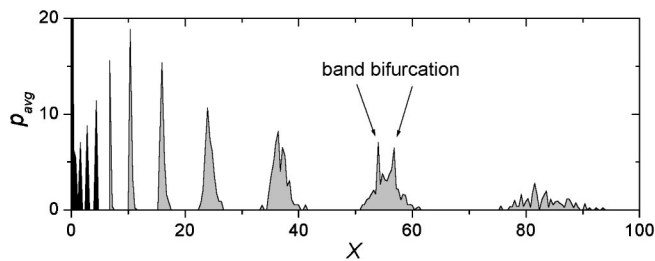


FIG. 3. Variation of the average amount of the precipitate in the diffusion column for $\Delta=0.2$. The distribution of the precipitate corresponds to the 100 independent simulations. The black and gray color correspond to the deterministic and the stochastic band positions, respectively.

(variation of the stochastic pattern structures and standard deviations with Δ) are in good agreement with the results of experimental findings.⁵⁻⁷

We observed an interesting phenomenon, a so-called spatial bifurcation of a single band into two bands, presented in Fig. 3. It should be noted that the peaks of the two bands are approximately two times higher than the peak between them, i.e., than that of the basis band. Recall that this band separation was obtained as an average of 100 simulation results and not by individual pattern evolution. Similar phenomenon has been observed in real experiments.^{5,7,26} See Fig. 9 in Ref. 7.

We have performed Gaussian fitting for the average amount of the precipitate depicted in Fig. 1. In some cases the fitting procedure did not converge because the data structure was not Gaussian. By increasing Δ , the variation of the fitted curves decreases for any fixed band number (n). In spite of the fact that increasing Δ implies higher concentration perturbations, at a given space position one can observe smaller variations of the band positions. Our results and findings are summarized in Table I.

IV. CONCLUSIONS

We have modeled stochastic pattern distribution using perturbed concentrations in a deterministic model. The precipitation process was based on the simplest approach, applied ion-product supersaturation theory (based on Ostwald's idea). Liesegang patterns in the simulations are found to be increasingly stochastic, in terms of reproducibility of the band locations and of band formation as the initial concentration difference, between the inner and outer electrolyte Δ is decreased. The numerical results on the spatial distribution of band locations are presented by an average of 100 runs to which in most cases Gaussian function can be fitted. In some cases, the fitting procedure was not possible far from the

TABLE I. Parameters of the fitted Gaussian curves. \bar{X}_n and $\bar{\sigma}_n$ denote the mean and the standard deviation of the empirical data of the position of the n th band, respectively. Notation “det” corresponds to the deterministic band positions and “(-,-)” yields the case, where the fitting procedure could not be performed.

Δ	$(\bar{X}_3, \bar{\sigma}_3)$	$(\bar{X}_4, \bar{\sigma}_4)$	$(\bar{X}_5, \bar{\sigma}_5)$	$(\bar{X}_6, \bar{\sigma}_6)$	$(\bar{X}_7, \bar{\sigma}_7)$	$(\bar{X}_8, \bar{\sigma}_8)$	$(\bar{X}_9, \bar{\sigma}_9)$	$(\bar{X}_{10}, \bar{\sigma}_{10})$	$(\bar{X}_{11}, \bar{\sigma}_{11})$
0.0	(4.32, 0.23)	(7.50, 0.23)	(12.7, 0.49)	(21.1, 0.91)	(34.5, 1.70)	(56.2, 4.97)	(-, -)	(-, -)	(-, -)
0.2	det	(4.51, 0.23)	(10.5, 0.13)	(16.0, 0.59)	(24.2, 1.27)	(36.6, 2.35)	(-, -)	(82.0, 3.52)	(-, -)
0.4	det	(5.34, 0.26)	(7.68, 0.10)	(11.1, 0.39)	(16.3, 0.66)	(23.5, 1.18)	(34.0, 2.31)	(48.8, 5.53)	(69.6, 4.32)
0.8	det	det	det	det	(14.1, 0.26)	(19.0, 0.50)	(25.7, 0.90)	(34.7, 1.30)	(46.7, 1.90)

junction point of the two electrolytes. Results of the simulations show that increasing Δ , the spatial distribution of the precipitate is more deterministic, nevertheless the amplitude of the maximal concentration perturbation is proportional to the square root of concentration. Δ exactly determines the pattern structure as pointed out in Ref. 7. Our model reproduces all experimental findings on pattern formation for low initial concentration gradient.⁵⁻⁷

ACKNOWLEDGMENTS

The authors are very grateful to Judit Zádor for helpful discussions. We acknowledge the support of the OTKA grant F03480 and the OMF B grant 00580/2003 (IKTA5-137) of the Hungarian Ministry of Education.

¹R. E. Liesegang, *Naturwiss. Wochenschr.* **11**, 353 (1896).

²R. Matalon and A. Packter, *J. Colloid Sci.* **10**, 46 (1955).

³T. Antal, M. Droz, J. Magnin, Z. Rácz, and M. Zrinyi, *J. Chem. Phys.* **109**, 9479 (1998).

⁴K. Jablczyński, *Bull. Soc. Chim. Fr.* **33**, 1592 (1923).

⁵S. Kai, S. C. Müller, and J. Ross, *J. Phys. Chem.* **87**, 806 (1983).

⁶S. Kai and S. C. Müller, *Sci. Form* **1**, 9 (1985).

⁷S. C. Müller and J. Ross, *J. Phys. Chem. A* **107**, 7997 (2003).

⁸L. Arnold, *On the Consistency of the Mathematical Models of Chemical Reactions, Dynamics of Synergetic Systems*, edited by H. Haken (Springer, Berlin, 1980).

⁹B. Chopard, P. Luthi, and M. Droz, *Phys. Rev. Lett.* **72**, 1384 (1994).

¹⁰B. Chopard, P. Luthi, and M. Droz, *J. Stat. Phys.* **76**, 661 (1994).

¹¹F. Izsák and I. Lagzi, *Chem. Phys. Lett.* **371**, 321 (2003).

¹²I. Lagzi and F. Izsák, *Phys. Chem. Chem. Phys.* **5**, 4144 (2003).

¹³G. Venzl and J. Ross, *J. Chem. Phys.* **77**, 1302 (1982).

¹⁴G. T. Dee, *Phys. Rev. Lett.* **57**, 275 (1986).

¹⁵M. E. LeVan and J. Ross, *J. Phys. Chem.* **91**, 6300 (1987).

¹⁶D. S. Chernavskii, A. A. Polezhaev, and S. C. Müller, *Physica D* **54**, 160 (1991).

¹⁷A. A. Polezhaev and S. Müller, *Chaos* **4**, 631 (1994).

¹⁸A. Büki, É. Kárpáti-Smidróczki, and M. Zrinyi, *J. Chem. Phys.* **103**, 10387 (1995).

¹⁹A. Büki, É. Kárpáti-Smidróczki, and M. Zrinyi, *Physica A* **220**, 357 (1995).

²⁰H.-J. Krug and H. Brandtstädter, *J. Phys. Chem. A* **103**, 7811 (1999).

²¹Z. Rácz, *Physica A* **274**, 50 (1999).

²²M. Chacron and I. L'Heureux, *Phys. Lett. A* **263**, 70 (1999).

²³T. Antal, M. Droz, J. Magnin, A. Pekalski, and Z. Rácz, *J. Chem. Phys.* **114**, 3770 (2001).

²⁴W. Ostwald, *Kolloid-Z.* **36**, 380 (1925).

²⁵H. W. Morse and G. W. Pierce, *Proc. Am. Acad. Arts Sci.* **38**, 625 (1903).

²⁶S. Kai, S. Higaki, H. Yamasaki, and T. Yamada, *Trans. IEE Jpn.* **107**, 1011 (1987).